

Chapter 2

Types of Nanoparticles Used in XLPE Systems



Karakkad P. Sajesh

1 Introduction

Polymer composites are a combination of two or more components of different phases that include polymers and fillers. These fillers belong to different geometries like fibrous, irregular flakes, spheres, circular, cubic and plate-like structures, etc., which can be continuous (long fibers) or discontinuous (short fibers, flakes, platelets) in nature [1]. Physically they are rigid materials, immiscible in polymer matrix in molten or solid states giving rise to different morphology. These fillers can be classified as inorganic and organic materials further based on their origin, fillers can be classified as natural and synthetic. The different classification of these fillers with examples has been summarized in Table 1.

The dispersion of fillers is homogeneously in the polymer matrix, in very small concentrations usually less than 10 wt% and when the particles are in the nanometer range, the materials are known as nanocomposites. The formation of interface zone between the polymer and nanoparticles makes the nanocomposite different from microcomposite. Hence, the unique properties of nanocomposites [2] give them the great potential for advanced applications. Various nanoparticles, such as nanoclays like montmorillonite, nano-oxides like TiO_2 , SiO_2 , Al_2O_3 , etc., semiconducting particles like SiC , ZnO , etc., have been widely studied due to their property of improving the performances of different thermoplastic and thermosetting polymers. Thus, the properties of nanocomposites are influenced by the nature of polymer matrix and filler used, their internal properties, size and shape of fillers, the surface functionalization, thickness of the filler surface, and interactions between the polymer matrix and fillers.

Cross-linked polyethylene (XLPE) which is an alternative to polyvinyl chloride (PVC), chlorinated polyvinyl chloride (CPVC), and copper tubing has an extensive

K. P. Sajesh (✉)

School of Chemical Sciences, Mahatma Gandhi University, Kottayam, Kerala 686560, India
e-mail: kp.sajesh@gmail.com

© Springer Nature Singapore Pte Ltd. 2021

J. Thomas et al. (eds.), *Crosslinkable Polyethylene Based Blends and Nanocomposites*, Materials Horizons: From Nature to Nanomaterials,
https://doi.org/10.1007/978-981-16-0486-7_2

Table 1 Classification of fillers and their examples

Classification	Chemical structure	Examples
Natural	Animal	Silk, wool, hair
	Mineral	Asbestos
	Cellulose	Wood, seed, leaf, fruit, grass
Synthetic	Inorganic	Oxides: TiO ₂ , SiO ₂ , Al ₂ O ₃ , ZnO, MgO,
		Hydroxides: Al(OH) ₃ , Mg(OH) ₂
		Metals: Al, Au, Ag, B, Sn, Cu, steel
		Silicates: asbestos, talc, mica, nanoclay, kaolin
		Salts: CaCO ₃ , BaSO ₄ , CaSO ₄ , etc.
		Carbides and nitrides: AlN, BN, SiC
	Organic	Carbon and graphite fibers and flakes, carbon nanotubes, carbon black, graphene, graphene oxide
		Synthetic polymers: polyester, polyamide, polyvinyl alcohol fibers

Adapted from [1]

range of applications due to its specific physical and chemical properties. It has very high enhanced properties when compared with ordinary polyethylene (PE). PE [3] itself is an insulating material due to its excellent dielectric strength, high insulation resistance, and a low dissipation factor. It being a commodity plastic with low cost, easy availability and processing has major application in household items, packaging, and insulation, net ropes, fishing rods, medical applications, etc., and being thermoplastic can be easily reprocessed. The main defect of PE is its limited temperature range. On increasing the temperature, it softens and begins to flow there by losing its critical physical properties. Cross-linking the PE increases the temperature range of the insulation without damaging its electrical properties. Both physical and chemical approaches [4] are followed by the scientific word in cross-linking the polyethylene. Some of the methods of cross-linking are given in Fig. 1.

Almost all types of polyethylene like linear low density polyethylene (LLDPE), low density polyethylene (LDPE), high density polyethylene (HDPE), etc., [5] are cross-linked to improve their properties. Upon cross-linking, the polymer changes from thermoplastic to thermosetting resulting in a polymer matrix which is durable. Also, cross-linking inhibits the flow of melt. XLPE is suitable for high-to-low voltage ranges thus surpassing other insulation materials like PVC, ethylene propylene rubber (EPR), and silicone rubbers. Cross-linking the polyethylene also enhances the chemical and oil resistance at elevated temperatures making it suitable for use as a low smoke zero halogen material, for natural gas and offshore oil applications, chemical transportation, and transportation of sewage and slurries [6]. It is widely used in pipework systems, hydronic radiant heating and cooling systems, domestic water piping, etc. It is a thermoset insulation [7] material for high tension electrical cables. Cross-linking of the polymer increases low-temperature

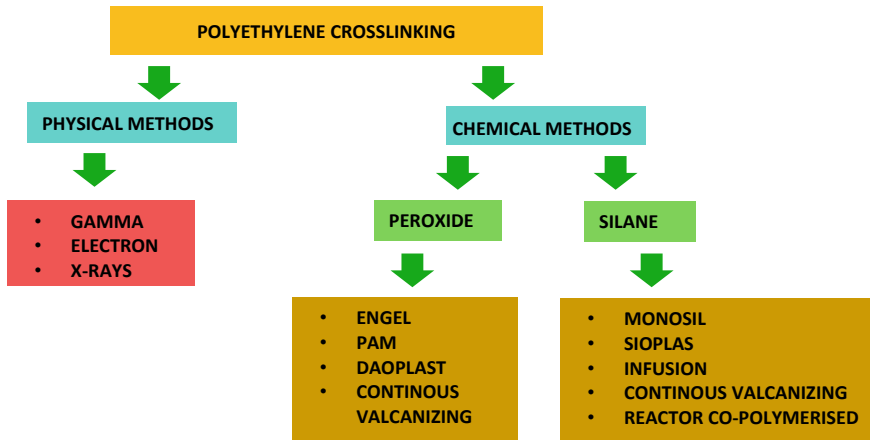


Fig. 1 Different methods for cross-linking polyethylene

impact strength, abrasion resistance, and environmental stress cracking resistance, reducing hardness and rigidity. The mechanical properties of the XLPE like greater tensile strength, elongation and impact resistances make it superior to other insulating materials. Even at very high temperatures, the XLPE insulation will not melt or drip. It is also characterized by the increased flow resistance and better aging property. XLPE also shows improved water tree resistance which is another benefit of XLPE insulating materials used for low voltage (LV) cables and medium voltage (MV) cables over PE insulating materials [8]. Thus, the replacement of LDPE with XLPE [9] increased the thermomechanical properties of insulators in power cables. As a result of cross-linking, the thermal stability and long-lasting operation in service was significantly increased and hence XLPE with the ability to withstand even short circuit for few seconds over 200 °C has a large extent of application. However, the degree of cross-linking varies from application to application. Table 2 gives the variation in the properties of PE upon cross-linking.

In spite of these advantages, XLPE faces certain drawbacks. The accumulation of space charge [10] inside them creates distortion of local electric field, giving acceleration to insulating aging, shortening the lifespan of the cable, etc. The advancement of nanotechnology in recent years has helped the scientific world in improving the properties of polymer through the introduction of nanocomposites [11, 12]. Nanocomposites, the multicomponent system, include a matrix and one or more than one dispersed fillers. They proved that the interface between nanoparticles and polymer matrix provides a great impact on the dielectric properties of the nanocomposite. Figure 2 gives the pathway involved in formation of XLPE nanocomposite from PE.

These nanocomposites find their applications in biomedical, clinical, and electrical fields. For example, in high voltage applications, nanodielectrics [13], etc. These polymer nanocomposites due to their potential benefits as dielectrics are

Table 2 Degree of change in the properties of PE upon cross-linking

Polyethylene properties	Change in properties on cross-linking of polyethylene
Density	No change or slight decrease
Melt index	Decrease
Molecular weight	Significant increase
Tensile strength	No change or slight increase
Elongation at break	Decrease
Impact resistance	Significant improvement
Abrasion resistance	Great improvement
Stress crack resistance	Great improvement
Elastic properties	Great improvement
Environmental stress crack resistance	Increase
Resistance to slow crack growth	Increase
Temperature resistance	Great improvement
Chemical resistance	Significant improvement

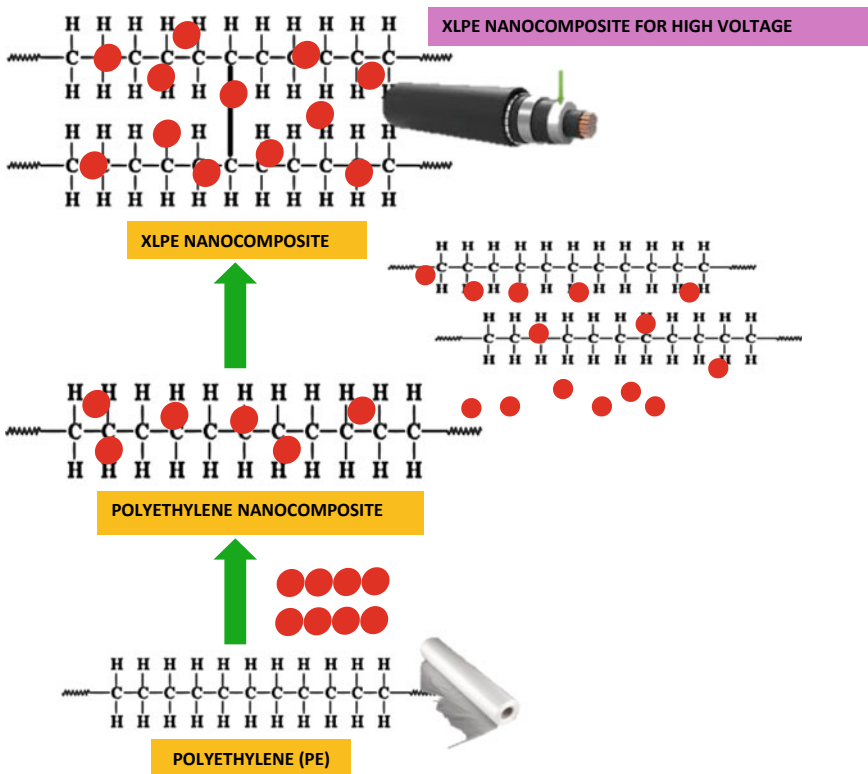


Fig. 2 Schematic representation of the pathway from PE to XLPE nanocomposites

gaining great attention as they have very much improved dielectric strength. The nanosized inclusion benefitted the electrical insulation with low dielectric loss. When there is disturbance in maintaining the applied voltage across the material in a stable manner without excess current flow, electrical breakdown occurs. The best candidate can be the cross-linked polyethylene nanocomposites which can work as an insulator with high breakdown strength resisting the breakdown mechanisms. Along with this, the filler size, material and aspect ratio, surface functionalization, filler grade, host material, type of synthesis, etc., affect the insulating capacity of nanocomposite. XLPE is thus the most widely used insulation polymer at high breakdown voltage. A large number of different nanomaterials of spherical shape have been applied as fillers for the formation of nanocomposites. They include metals like Al, Fe, Au, metal oxides like Al_2O_3 , Fe_3O_4 , ZnO, TiO_2 , semiconductors like PbS and CdS, metalloid oxides like SiO_2 , etc. There are also other types of nanofillers like carbon nanotubes and cellulose whiskers, fillers of the form of sheets such as graphite, layered SiO_2 including montmorillonite, hectorite, saponite, etc. Thus, cross-linked polyethylene nanocomposites with organic/inorganic nanoparticle fillers exhibit enhanced electrical breakdown strength compared to their unfilled or micron filled members and is the newly emerging dielectric materials which over heads the existing ones. The development of insulation cables since 1913 is described in Fig. 3. Some of the important nanoparticles in XLPE nanocomposites are discussed in detail in this chapter.

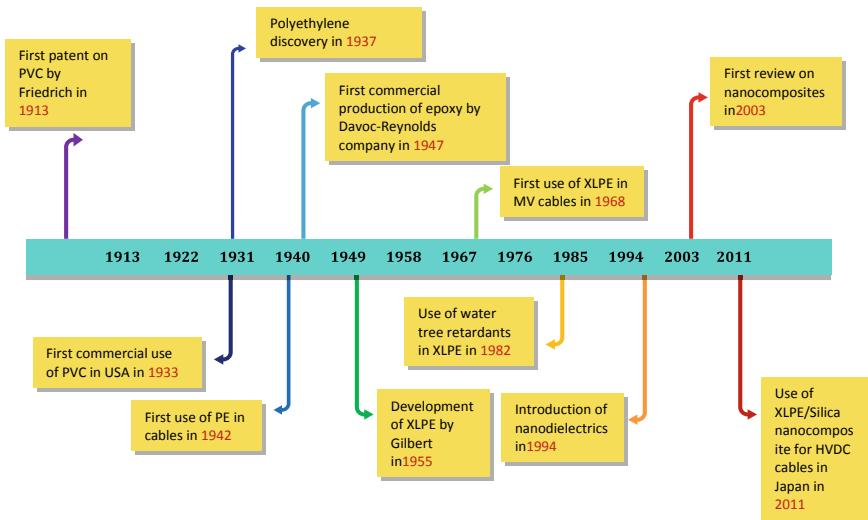


Fig. 3 Development of insulation cables since 1913

2 XLPE Nanocomposites

Nanomaterials have been attaining attraction recently by the researchers in the field of dielectrics and electrical insulation [14]. Nanocomposites are materials in which the polymer matrix is filled with inorganic particles that are nanosize in nature. The XLPE as insulation material for DC cables has been improved by the addition of nanosized inorganic particles [15]. This technology guarantees the improvement in the insulating performance of the polymer. Some of the main applications of XLPE nanocomposites are pictorially represented in Fig. 4. A few of the nanofillers in XLPE are discussed in this chapter which includes SiO₂, TiO₂, Al₂O₃, Clay, MgO, GO, BNNs, etc.

3 SiO₂ Nanoparticles in XLPE Matrix (SiO₂/XLPE Nanocomposite)

A number of experimental studies performed in recent years indicate that the nanoparticles can be used as a promising filler in power cable insulation which suppresses the growth of electrical tree and prevents the degradation of polymer matrix [16–18]. Among the different nanofillers used, SiO₂ has been widely studied with different polymer matrices due to their mild and easy process involved in its preparation. Hence, a lot of efforts have been applied on the investigation of the polymer/SiO₂ nanocomposites to modify their properties for the special applications. The experimental studies by Tanaka et al. using XLPE and fumed silica (SiO₂) showed that SiO₂ additives in XLPE matrix could be largely applied in the fields of extruded high voltage (HV) and extra high voltage (EHV) cables [19].

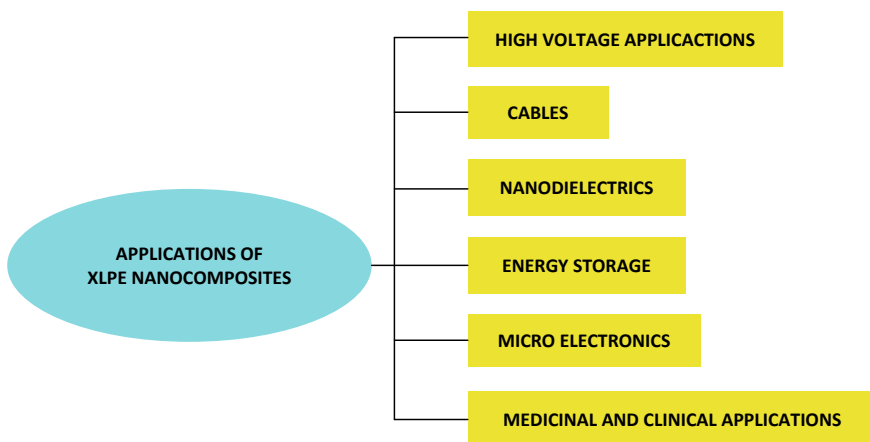


Fig. 4 Applications of XLPE nanocomposites

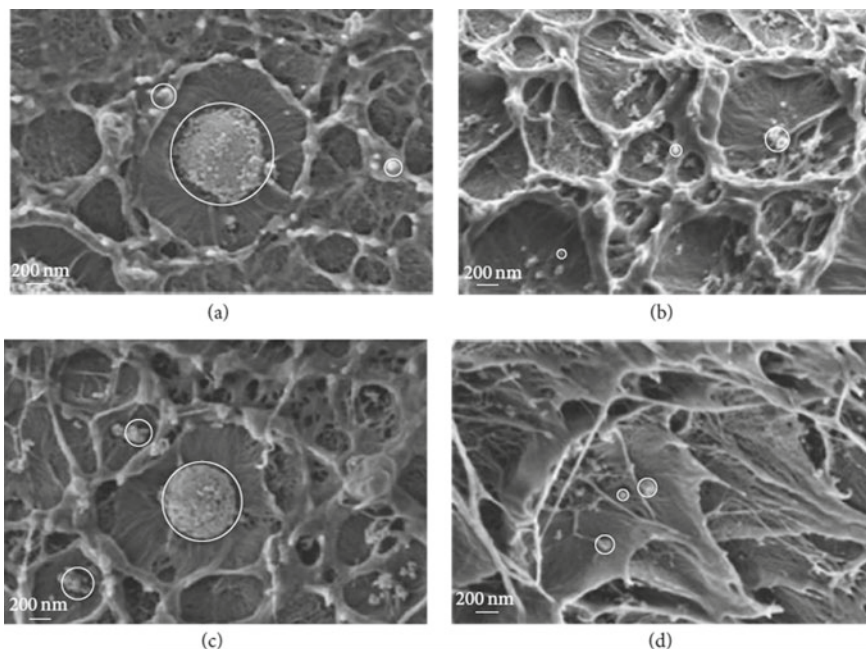


Fig. 5 SEM of TiO_2/XLPE . **a** UN- TiO_2/XLPE (1 wt%), **b** MDOS- TiO_2/XLPE (1 wt%), **c** UN- TiO_2/XLPE (5 wt%), and **d** MDOS TiO_2/XLPE (5 wt%). Adapted from [10]

Unfilled XLPE, XLPE filled with 5% non-functionalized fumed silica nanofiller, and XLPE filled with 5% functionalized fumed silica nanofiller were used for their study. In order to study the distribution of fillers, they used SEM. The unfilled sample of XLPE showed no significant morphological features when examined by SEM and thus compared to the SEM of untreated filler sample it was evident that the filler particles span a wide size approximately 300 nm to 30 μm and are uniformly distributed throughout the material. The SEM micrographs of the morphology of peroxide cross-linked XLPE, XLPE with untreated nanofiller and XLPE with treated nanofiller has also been obtained. DSC measurements gave the melting behavior of the XLPE samples. All melting traces were obtained at a heating rate of 10 K min^{-1} . Here, both of the treated and untreated nanofiller nanocomposites melted at a significantly lower temperature of 102 $^\circ\text{C}$ than the unfilled system of 104 $^\circ\text{C}$. Thus, the nanoparticles reduce the formation of crystalline order due to the presence of nanoparticle interactions with the polymer. Gas chromatography studies showed that cross-linking residues diminishes by the heat treatment at 80 $^\circ\text{C}$ for a week in vacuum, whereas by heat treatment at 60 $^\circ\text{C}$ for a week some might remain. A three-terminal cell system with its gold coated electrodes was used in DC charging measurements. At an electric field of 20 kV/mm a steady-state current was obtained. The DC current density data between unfilled XLPE filled XLPE before and after heat treatment shows that the DC conductivity is decreased with XLPE

filled with 5 wt% silica nanofillers. Heat treatment for 5 days at 80 °C causes much more reduction in DC conductivity, except for unfilled XLPE. Hence, nanofillers act as nucleation items for by-products and contaminants. The space charge measurements were performed by different methods like pulsed electroacoustic (PEA) and thermal step (TSM) method. Small amount of heterocharge existed for filled XLPE and homocharge for unfilled XLPE with thin sample of 85 μm thickness at a field of 50 kV/mm. Montanari (low field) PEA results gave lower space charge accumulation for filled XLPE samples than unfilled one and the lowest value was obtained surface-treated nanofiller XLPE. They also showed the reduction in space charge for filled XLPE on thermal treatment. Tanaka and Ohki (high field) PEA results gave evidence for heterospace charge in unfilled XLPE and homospace charge in filled XLPE. Y. Tanaka (high field) PEA results gave no significant space charge for 1 mm thick samples at the field 30 and 40 kV/mm. Castellon (low field) TSM results showed that filled XLPE accumulates less space charge than unfilled XLPE and functionalized filler filled XLPE exhibited the lowest electric field and double injection occurs here. Thus, in short heterocharge is formed for unfilled XLPE which reduces on addition of nanofiller. Also, shorttime breakdown (BD) strength and impulse BD strength are unaffected by the addition of nanofillers. And partial discharge (PD) resistance is markedly improved by nanofiller addition. As a result of their wide studies, SiO_2/XLPE nanocomposite can be considered as one of the best examples of modified polymer with extensive interface regions and having enhanced synergistic or unique dielectric properties.

Apart from these kinds of studies, there are also studies on functionalization of SiO_2/XLPE nanocomposites that results in modified properties. The use of a titanate coupling agent (TC9) and 3-(methacryloyloxy)propyltrimethoxysilane (KH570) by Zhang et al. to modify the SiO_2 surface showed an improved DC conductivity, dielectric, and space charge properties in XLPE/ SiO_2 nanocomposites [20]. They used XLPE mixed with unmodified SiO_2 nanoparticles (XLPE/UN- SiO_2), XLPE mixed with surface-modified SiO_2 nanoparticles by KH570 coupling agent (XLPE/KH570- SiO_2), and XLPE mixed with surface-modified SiO_2 nanoparticles by TC9 coupling agent (XLPE/TC9- SiO_2) for studies to examine the influence of different nanoparticle surface modifications on interface effects. They could conclude from FESEM that the XLPE/UN- SiO_2 nanocomposites face agglomerate problems whereas XLPE/KH570- SiO_2 and XLPE/TC9- SiO_2 showed a decrease in agglomeration. The FESEM results show the decrease in agglomeration with KH570 coupling agent (both size and number), compared to XLPE/UN- SiO_2 nanocomposites. The agglomerate size of SiO_2 nanoparticles ranged from several ten nm to several hundred nm. Further decrease in the size of agglomerates was reported with TC9 coupling agent. They also concluded the improvement in surface hydrophobicity of SiO_2 nanoparticles upon surface modification and the decrease in DC conductivity in the XLPE/KH570- SiO_2 and XLPE/TC9- SiO_2 nanocomposites. DC polarization current measurements were done using three-terminal cell system at an electric field of 10 kV/mm lasting for 10 min and four temperatures 20, 40, 60, and 80 °C were chosen. However, with rise in temperature, the DC conductivity increases much more slowly than the unmodified nanocomposites. FTIR studies

were also adopted to study the variation on surface modification. The reflection peaks of XLPE/KH570-SiO₂ and XLPE/TC9-SiO₂ nanocomposites are almost similar and larger than XLPE and XLPE/UN-SiO₂ nanocomposite. This was due to surface modification of SiO₂ nanoparticles. Similarly the trap depth and trap density for modified nanocomposite are more than unmodified one. The surface modification of SiO₂/XLPE nanocomposites and their influence on the DC breakdown and space charge have also been studied by Zhang et al. in 2014. They utilized a titanate and vinylsilane coupling agents having non-polar functional groups as the surface modifiers of SiO₂ nanoparticles. They proved that the surface modification of SiO₂ improved the DC breakdown under different temperature and XLPE/VISiO₂ [21, 22] nanocomposite processed highest DC breakdown strength with low dispersibility. They also showed that the introduction of organic surface modification leads to the formation of deeper trap sites which supports the suppress and greater movement of space charges. In 2017, Zheng et al. also reported the making of matrix compatible PSMA(poly(stearyl methacrylate)) brush grafted SiO₂/XLPE nanocomposite that suppresses the space charge and internal field distortion giving a large range of external DC field from -30 to -100 kV/mm at room temperature. They made use of four samples for their study, namely XLPE, UN-SiO₂/XLPE, free-PSMA/XLPE, and PSMA-SiO₂/XLPE. The uniform distribution of the nanoparticle contributed to the increase in the interfacial volume thus improving its efficiency. Space charge distribution under 30 kV/mm was studied using a pulsed electroacoustic method at room temperature. Just after polarization, a decrease in the positive charge on the anode was observed for all samples. After polarization for 30 min in XLPE, net positive charge is distributed across the sample. Approximately 7 C/m³ of positive carriers accumulated in the bulk of UN-SiO₂/XLPE nanocomposites and smaller quantity of positive carriers accumulated in free-PSMA/XLPE composites. On the other hand, no charge was observed in the bulk of PSMA-SiO₂/XLPE nanocomposites even after 60 min. The ability of the nanocomposites in suppressing space charge was done by applying a field of approximately 100 kV/mm. This resulted in forming a positive charge packet in XLPE that slowed down during the 60 min transit across the insulation and a smaller positive charge packet in UN-SiO₂/XLPE nanocomposite that slowly moved a distance of approximately 50 μm. In the case of free-PSMA/XLPE, initially bipolar charge injection and transport were observed which were then followed by the appearance of a negative charge packet that transited and recombined with positive carriers near the anode. Comparison of the charge trapping ability of XLPE and its composites were studied using TSC measurements. The PSMA-SiO₂/XLPE system showed an exponential growth with the temperature in the TSC spectra that reached 12.7 pA at 90 °C due to traps in the interfacial region and an increase in the nanoparticle matrix interfacial volume. Furthermore, the large TSC in the well-dispersed system at higher temperature suggests that the newly introduced chemical defects act as deep trapping sites. Furthermore, the DC breakdown test was carried out with ball-plane electrodes according to International Electrotechnical Commission (IEC) standard 60243-2: 2001 and DC BDS was assessed by the two parameter Weibull distribution. The results showed that the

lowest breakdown strength was found for agglomerated UN-SiO₂/XLPE system and was the relatively well-dispersed system that outperformed free XLPE. Moreover, the addition of free-PSMA chains did enhance the DC BDS. Also, it has been seen that XLPE encountered a severely increasing trend of field distortion due to the charge evolution. When UN-SiO₂ NPs were incorporated into XLPE field, distortion could be improved but the agglomerates could remain as defects and lead to lower breakdown strengths. The free-PSMA/XLPE group showed a better performance than UN-SiO₂/XLPE NCs with regard to the field distortion. The maximum internal field distortion of PSMA-SiO₂/XLPE NCs was only 9.5% under -100 kV/mm and less than 10.6% for DC fields from -30 to -100 kV/mm. This shows that PSMA-SiO₂/XLPE NCs has a tremendous potential for improving HVDC power cable insulation.

The space charge distribution also depends on the nanocomposite thickness. The investigation on thickness dependence and space charge distribution in unfilled XLPE and SiO₂/XLPE nanocomposites were done by Lv et al. [23] and they could see that the SiO₂/XLPE nanocomposites sample with low thickness accumulated larger heterocharge compared to thicker sample.

Surface modification of SiO₂/XLPE nanocomposites has been widely studied by the scientific world as it offers a major application to high-voltage cables. Roy et al. studied the surface modification of SiO₂/XLPE nanocomposite and its electrical applications by modifying the SiO₂ surface using triethoxyvinylsilane (TES), n-(2-aminoethyl)3aminopropyltrimethoxysilane (AEAPS) and hexamethyldisilazane (HMDS) [24]. The DC breakdown field was 1.45, 1.25, and 1.65 times as neat XLPE for XLPE/AEAPSSiO₂, XLPE/HMDSSSiO₂, and XLPE/TESSSiO₂ nanocomposites, respectively. Sharad et al. also studied the surface modification of SiO₂/XLPE nanocomposite by using octylsilane-modified silica nanofillers [25] and studied the partial discharge characteristics of the nanocomposites. Their studies using the differential scanning calorimetry (DSC), thermogravimetric analysis (TGA), Fourier transform infrared (FTIR), and contact angle measurement proved that the addition of nanosilica resulted in changing the melting point, thermal degradation temperature, heat of fusion, bonding structure, and the contact angle of the polymer. Surface modification were also done by Jin Kaihao et al. in 2018 where the SiO₂ was modified with γ -aminopropyltriethoxysilane KH550, γ -(2,3-epoxypropoxy) propyltrimethoxysilane (KH560), and triethoxyvinylsilane (A-151) [26]. They studied the space charge characteristics of nanocomposites using pulse electroacoustic methods (PEA) and obtained beneficial properties in the modified samples.

Apart from the experimental studies, theoretical calculations have also been carried out relating the nanocomposites. These studies mainly focus on the electronic interaction between the SiO₂ fillers and the polymer and also aim in designing the SiO₂ particle with greater efficiency with improved structure. The stabilizing effect of the double layer around the SiO₂ nanocluster in electron trapping has been studied theoretically using the quantum mechanics/molecular dynamics (QM/MD) simulations [27] based on a self-consistent charge density functional tight-binding (SCC-DFTB) method by Han et al. The results of their

calculations for the high ionization potential (IP) and electron affinity (EA) of SiO₂ nanocluster indicate that it is a promising member for reducing electrical treeing.

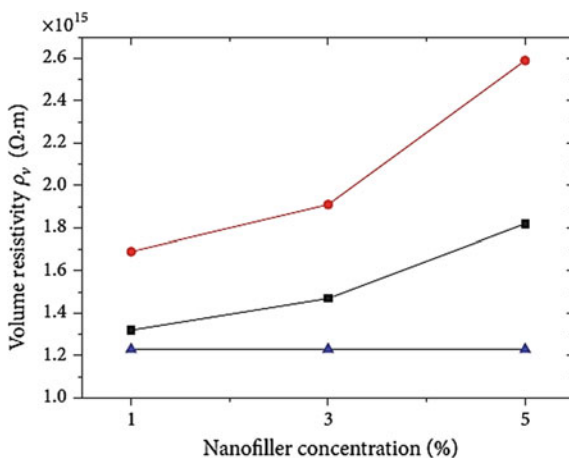
One of the most abundant economic mineral α -SiO₂ known as α -quartz is found to have a wide range of applications beginning from high-frequency devices, cellular and satellite network, quartz crystal microbalance, etc. [28–31]. Different models with the modified surfaces for increasing the rate of reaction developing the adsorption effect have also been proposed. For example, the six-member ring and a triangle-like structured dense model [32, 33], the hydroxylated model giving silanol groups [34], the one with the N or B-doped models [35–38], etc., and these properties of α -SiO₂ affect its interfacial interaction with XLPE thus increasing the performance of SiO₂/XLPE nanocomposites in power cable insulation. Zheng et al. used the computational calculations to study the electrical tree inhibiting mechanism of the SiO₂ fillers with nanosize and various modified surface structures [39]. They used their studies to determine the ability of particles in trapping hot electrons and preventing space charge. They applied the density functional theory (DFT) calculations using the Vienna Ab Initio Simulation Package (VASP) [40–42] with Perdew–Burke–Ernzerhof (PBE) functional [43]. They used the DFT-D2 method to measure the van der Waals interaction and the projected augmented wave (PAW) method [44] to study the interaction between valence electrons and ion cores. They aimed to establish the mechanism involved in improving the anti-aging properties and performance of XLPE by the addition of SiO₂ particles. They analyzed the electrical properties of a series of SiO₂/XLPE nanocomposites on the basis of surface structures, interfacial interaction, H migration activity, and space charge behavior. They concluded the reduction in space charge accumulation and inhibition of electrical treeing on addition of SiO₂ nanosized fillers which increases the power of power cable insulation by trapping hot electrons and limiting the movement of cross-linked polyethylene. They also proved that the incompletely hydroxylated SiO₂ or surfaces with boron doping are not very much effective in insulation cables as they destroy the XLPE chain and also supports the H migration reaction. They showed that the SiO₂ N-doped having a completely hydroxylated surface is the most effective nanocomposite among the different species studied. Their abilities of adsorption to XLPE and transferring charge and the weak chemical activity leads to this efficiency. The studies of Zheng et al. can also lead to the designing of other potential surface-modified SiO₂/XLPE nanocomposites.

A large number of other different studies have been performed in this area focusing on the improvement of the properties of the nanocomposites. These experimental and theoretical studies make SiO₂/XLPE and its surface-modified nanocomposite members a promising material in cables and high-voltage applications.

4 TiO₂ Nanoparticles in XLPE Matrix (TiO₂/XLPE Nanocomposite)

Similar to SiO₂ nanofillers in XLPE, the TiO₂ as nanofillers and their surface modification has also been studied to some extent. The major benefit of titanium dioxide over common nanocomposites is the value of its permittivity constant. The relative permittivity of this material reaches to a level of 100, which is the main reason for attracting many experts in discovering the extraordinary properties of titanium dioxide also called titania. Wang et al. studied the space charge characteristics of the unmodified TiO₂/XLPE [10] nanocomposites and the TiO₂/XLPE modified by dimethyloctylsilane (DMOS) coupling agent where different mass concentrations of coupling agent, 1, 3, and 5 wt% were added in order to determine and modify the properties of TiO₂/XLPE nanocomposite and provide a reasonable explanation of the experimental phenomenon. The experimental techniques like scanning electron microscopy (SEM), volume resistivity testing, and PEA measurements were used for their studies. Interpretation from SEM results showed that the coupling agent DMOS improved the compatibility between TiO₂ nanoparticles and XLPE matrix to some extent and also caused the reduction in agglomeration of TiO₂ nanoparticles compared with unmodified sample. Along with this, the volume resistivity tests were also carried out to analyze the movement of carriers. TiO₂/XLPE nanocomposites had a greater volume resistivity compared to pure XLPE which increased with increasing the filler concentrations. The results of volume resistivity of pure XLPE and TiO₂/XLPE are given in Fig. 6. The PEA method was also used to determine the space charge characteristics of TiO₂/XLPE nanocomposite. They showed that space charge accumulation reduced with increase of TiO₂ nanofiller and also there was an improvement in electric field distribution. The homocharge injection was more predominant in MDOSTiO₂/XLPE than in unmodified one and decreased with increase in filling. The SEM images of TiO₂/

Fig. 6 Volume resistivity of pure-XLPE and TiO₂/XLPE. Adapted from [10]



XLPE, UN-TiO₂/XLPE (1 wt%), MDOS-TiO₂/XLPE (1 wt%), UN-TiO₂/XLPE (5 wt%), and MDOSTiO₂/XLPE (5 wt%) are shown in Fig. 5.

They showed that MDOS coupling agent improved TiO₂ nanoparticle dispersion and reduced the extent of agglomeration of TiO₂ nanoparticles in XLPE matrix. The order of volume resistivity of three samples is pure XLPE < UN-TiO₂/XLPE < MDOS-TiO₂/XLPE. Their explanation was that MDOS-TiO₂/XLPE nanocomposite had more traps than UN-TiO₂/XLPE, thus capturing more carriers, and the MDOS-TiO₂/XLPE nanocomposite had the largest volume resistivity. From PEA measurements, they showed that TiO₂ nanoparticles largely influenced the space charge accumulation behavior and the DC electric field improved the electric field distribution in TiO₂/XLPE to a large extent.

Wang et al. in 2016 also studied the dielectric properties of TiO₂/XLPE nanocomposites having different mass concentrations of 1, 3, and 5 wt% of TiO₂ [45]. They showed the greater volume resistivity of TiO₂/XLPE nanocomposites compared to XLPE. The TiO₂/XLPE nanocomposites had lower permittivity, low dielectric dissipation, which increased with increase in filling concentrations and decreased with the measured frequency.

Aishwarya S Nair et al. conducted a simulation study to determine the effect of water treeing in XLPE nanocomposites [46]. They showed that common XLPE had a higher electric stress from water treeing and differ from XLPE mixed with titanium dioxide. A two-dimensional single core cable model which was developed using COMSOL MULTIPHYSICS software and electric field distribution was analyzed with the help of finite element method (FEM). The relative permittivity values were changed with respect to the material. Depending on the electric field distribution, water tree was observed. They studied the electrical field distribution and electrical stress experienced in the presence of void, with and without the incorporation of nanoparticles. The duration of the time taken for the initiation of water treeing was found to be prolonged in the presence of nanoparticles. They chose four types of nanofillers namely nanosized titanium, silica, alumina, and nanoclay with XLPE as the base polymer with 2.5 and 15 wt% loading and discarded the higher weight percentage in order to avoid agglomeration. They concluded that the presence of water voids caused more stress on the edges of the water voids due to the high permittivity difference between the XPLE material and water voids. This high stress created a conducting path along the electric field direction resulting in the representation of water tree as a rectangular channel. However, the high electric field path through the insulation led to mechanical damage and insulation breakdown. They showed that the electric field stress inside the nanofiller is lower than that of interface in the presence or absence of water voids. They also added that the nanofillers having high permittivity leads to lower stress when compared to fillers having lower permittivity. Thus, the water treeing process leading to the breakdown of dielectric material was inhibited due to the lower electric stress inside the nanofillers and moves toward maximum stress at the interface points in the nanocomposite material. In the same year, an experimental test was conducted by few researchers; it was found out that the XLPE with titanium dioxide as nanofillers recorded a higher resistivity compared to standard XLPE.

These studies can prove that TiO_2 nanoparticle with XLPE can prove to be a promising member in the nanocomposite material though not as much as SiO_2/XLPE nanocomposite. However, very little studies have been performed relating to TiO_2 with XLPE when compared with SiO_2 with XLPE and hence would require greater attempts of research for a better application of TiO_2 .

5 Organic Montmorillonite Nanoparticles in XLPE Matrix (OMMT/XLPE Nanocomposite)

Montmorillonite (MMT) [47] is a type of layered silicate with two-dimensional nanostructure. Only when it is intercalated with polymer or attains exfoliated dispersion, the composite gives excellent performance. Li et al. investigated the dielectric properties of XLPE/montmorillonite nanocomposites, using two organic intercalants, namely octadecyl quaternary ammonium salt (OMMT1) and double octadecyl benzyl quaternary ammonium salt (OMMT2), each having two long alkyl chains. They also used ethylene vinyl acetate (EVA) that acts as the compatibilizer on this system. The alkane chain part of EVA is compatible with PE/XLPE, and the carboxylic portion of EVA is compatible with OMMT. The organic montmorillonite (OMMT) particles are treated with OMMT1 and OMMT2 and were blended with cross-linked polyethylene to prepare the nanocomposites. XLPE/OMMT composite was obtained by adding a certain proportion of organically modified OMMT1 and OMMT2 into XLPE and was melt blended using a torque rheometer. XLPE/EVA/OMMT composite was obtained by adding the organically modified OMMT1 and OMMT2, polymeric compatibilizer, and the low density polyethylene at a certain proportion for melt blending in the torque rheometer. The specimens under study include XLPE/OMMT1, XLPE/OMMT2, XLPE, XLPE/EVA/OMMT1, and XLPE/EVA/OMMT2. In XLPE/EVA/OMMT1, the interlayer spacing is further enlarged upon the addition of EVA compatibilizer and the layer spacing increases from 3.47 to 3.92 nm.

The variation rate represents the intercalation efficiency. From the morphological studies, they showed the easier intercalation of polyethylene to the OMMT1 layer. The presence of EVA to XLPE/OMMT1 showed a strong interaction at the interface and was free from voids giving excellent nanosized dispersion. However, in the case of OMMT2, the system gave poor intercalation between polyethylene and the OMMT2 layer and no microscale dispersion was observed. The introduction of EVA in XLPE/OMMT2 reduced the agglomeration but not to full extent due to the bulk structure of OMMT2. The dielectric properties of XLPE/OMMT composites were studied using broadband dielectric spectroscopy with a frequency range from 10^{-2} to 10^6 . The dielectric constants of XLPE/OMMT and XLPE/EVA/OMMT nanocomposites were found to decrease with an increase in frequency, and the dielectric constant of the XLPE/EVA/OMMT1 composite was lower than that of XLPE/EVA/OMMT2 due to the melt intercalation of OMMT1 which was well

attained when octadecyl quaternary ammonium salt was used as the intercalant in this system. Hydrogen bonding between the carboxyl parts of EVA was generated by the intercalant present on the surface of the nanocomposite and yields an intense interfacial force. This created difficulty in the turning direction polarization under an applied electric field and thus giving a low polarization rate and dielectric constant. The dielectric loss of neat XLPE remained constant. The accumulation of OMMT2 gave higher loss peak values compared with the accumulation of OMMT1. In the case of OMMT2, two apparent dielectric loss peaks appeared with or without the addition of EVA in the frequency range of 10^2 – 10^5 Hz and in OMMT1 the dielectric loss peak was observed at around 10^4 Hz. The structural difference of two intercalants and their dispersion on the XLPE matrix is the main reason for the difference in the loss peak values of the nanocomposites. The presence of strong interface interaction found between the OMMT layers and XLPE created the controlled segmental movement of the polymer decreasing the molecular polarization ability and thus reducing the dielectric constant and dielectric loss. In XLPE/OMMT nanocomposite, the increase of the melting point system and the broadening of the melting temperature range are closely related to the intercalation efficiency of matrix resin molecules into OMMT. OMMT1 has a greater influence on the melting point and the melting temperature range of the nanocomposites. Thus, OMMT1 has a greater impact on the degree of crystallization and crystalline morphology of the composites than OMMT2. Montmorillonite thus quickens the nucleation in XLPE/OMMT composite. On the other hand, enhanced interfacial interaction and the use of EVA reduce the overall crystallization rate. The use of EVA makes the OMMT and the matrix polymer to be well bounded at the interface. For OMMT1, the PE chains get easily intercalated into the layers and for OMMT2, and the PE was not intercalated and hence the dispersion was only in micron scale. The agglomerated OMMT2 could break away from the PE matrix upon fracture. As the OMMT2 particles are extracted from the matrix, it creates voids. The remaining part of the OMMT2 remains as agglomerate.

Analysis of structure and performance was done with the aid of XRD, DSC, and DMA. These studies show that OMMT are a class of intercalating nanocomposite material with good intercalation. In the rubber state, the system can be completely melted without destroying the interface effect between polymer and nanoparticles that restricts the chain segment movement giving the modulus of elasticity of more than 10^7 MPa. It shows that the addition of OMMT increases the storage modulus of all nanocomposites under a high temperature whose extent depends on the intercalation of polyethylene chain into the montmorillonite. This studies shows that the nanocomposites with good intercalation can improve the storage modulus of XLPE at high temperature.

The dielectric property studies conducted by Li et al. also demonstrate that the addition of OMMT increases the relative dielectric constant of XLPE/OMMT composite. The composites with OMMT1 and OMMT2 are represented by single dielectric loss peak and double dielectric loss peak in the high frequency range, respectively. With increasing temperature, the width of the double peaks increases, the molecular chain segment motion is restricted by the interface interactions, the

distribution of relaxation time widens such that the low-frequency peaks are diffused to a greater extent in the low frequency band. The intercalant of octadecyl quaternary ammonium salt enables a good compatibility between OMMT1 and the matrix resin. The dielectric spectrum displays the single-component dielectric loss peak. Thus, the dielectric constant and dielectric loss of nanocomposite depend on the degree of intercalation in the broadband range. Hence, the higher the degree of intercalation, the lower is the dielectric constant and dielectric loss. And also the dispersion of nanoparticles in matrix resin in the presence of compatibilizer depends on how the compatibilizer matches with the organic intercalants.

Thus, organic intercalants also form an important class of nanocomposites which depends on its performance. Its structure and performance are the keys to design the high-performance polymer nanocomposites.

6 Magnesium Oxide Nanoparticles in XLPE Matrix (MgO/XLPE Nanocomposite)

In addition to SiO_2 , TiO_2 , and montmorillonite particles, MgO particles can also perform its duty as nanomaterial in XLPE nanocomposites. In order to investigate the effect of nano-MgO [48] addition on grounded DC tree in cross-linked polyethylene (XLPE), comparative tree experiments were performed using XLPE and 0.5 wt% MgO/XLPE nanocomposite by periodic prestress-grounding in a needle-plane system by Wang et al. They conducted the space charge measurement using pulsed electroacoustic (PEA) method on both kinds of samples. The MgO/XLPE nanocomposite exhibited higher 50% tree inception voltage in the tree experiment. The results gave more homocharge injection in XLPE which hinders the generation of electrical tree. The MgO/XLPE nanocomposite shows shorter average tree length and width under positive voltages that result in slower tree propagation. Also, the average tree length–width ratio in MgO/XLPE nanocomposite decreases faster with increasing positive voltage. Two kinds of samples were prepared by Wang et al. for their studies, one is pure XLPE, and the other is 0.5 wt % MgO/XLPE nanocomposite. Both the samples were subjected to the grounded DC tree experiments under different polarities at room temperature. The sample placed in a glass container was immersed in pure silicon oil. The ten needles were connected by the copper wire. The DC voltage was provided with a half-wave rectifier. The experiment was done by periodic prestress-grounding, i.e., applying a DC voltage for 3 min and then grounding for 2 s, repeating for 20 times like this. Then the sliced sample was observed under microscope. Under each voltage, one sample with ten needles was tested for each material. Space charge distribution of the samples was measured using a PEA measurement system at room temperature. The upper electrode was set to be a semiconductive material and the lower electrode to be aluminum. The applied electric fields were 10, 20, 30, 40, and 50 kV/mm. The space charge distribution was measured during each electric field applying for

30 min. The ratio between the number of needles with trees and the total number of needles is defined as the tree initiation ratio. And this ratio was found to increase with the increase of voltage, and the tree initiation ratio of MgO/XLPE nanocomposite is lower than XLPE under the same voltage. The 50% tree inception voltage of MgO/XLPE nanocomposite is higher than that of XLPE. They provided relation between the positive voltage and tree initiation ratio, average tree length and average width of the tree. When the DC voltages were negative no obvious change in tree initiation ratio with the increase of voltage was observed. With the increase of voltage, the average tree length increases, and it increases faster under positive voltages. Also, the average tree length under positive voltage is always greater than that under negative voltage. We can also recognize that the average tree length of XLPE is greater than that of MgO/XLPE nanocomposite under the same positive voltage. When the voltage is negative and lower than 29 kV, there is no significant difference in average tree length between the two samples. When it is higher than 29 kV, the average tree length of XLPE is a bit greater than that of MgO/XLPE nanocomposite. With the increase in voltage, the average tree width increases, and the increase is faster under positive voltages. When the voltage is lower than 26 kV, the average tree width of MgO/XLPE nanocomposite under negative voltage is greater than that under positive voltage. When the voltage is higher than 26 kV, the average tree width of both samples under positive voltage is greater than that under negative voltage. When the voltage is positive, the average tree width of XLPE is always greater than that of MgO/XLPE nanocomposite under the same voltage. When the voltage is negative and lower than 32 kV, the average tree width in XLPE is smaller than that in MgO/XLPE nanocomposite. When the negative voltage increases to 35 kV, the average tree width in XLPE is a little bit greater than that in MgO/XLPE nanocomposite. When the voltage is positive, the average tree length–width ratio of both samples decreases with the voltage increasing, indicating that the tree grows not only lengthways, but also laterally. Also, when the voltage is positive, the decrease of average tree length–width ratio of MgO/XLPE nanocomposite is faster than that of XLPE. And when the voltage is lower than 29 kV, the average tree length–width ratio of MgO/XLPE nanocomposite is always greater than that of XLPE. However, when the positive voltage increases to 29 kV, the average tree length–width ratio of XLPE exceeds that of MgO/XLPE nanocomposite. Hence, the lateral branches of electrical tree in MgO/XLPE nanocomposite is very short compared with the lengthways branches when the voltage is low and grow significantly with the voltage increasing. It can be observed that in XLPE, a huge amount of homocharge accumulates near both electrodes. The amount of homocharge increases with the increasing of applied electric field. As for MgO/XLPE nanocomposite, heterocharge is observed near both electrodes and it increases with the increasing of applied electric field. It can be concluded that the homocharge injection is more serious in XLPE than in MgO/XLPE nanocomposite. The heterocharge accumulation in the latter one may due to the dissociation of the impurities introduced by nanoparticles. The result of space charge measurement shows that the homocharge injection is more serious in XLPE than in MgO/XLPE nanocomposite when under

the same voltage. Thus, it can be inferred that when applying a DC voltage during the tree experiment, more homocharge is injected and accumulates around the needle tip in XLPE than in MgO/XLPE nanocomposite. Hence, the local electric strength produced by the injected charge and the electric mechanical energy released by the charge returning at grounding in XLPE is stronger than those in MgO/XLPE nanocomposite. Besides, in MgO/XLPE nanocomposite, the nanoparticles act as traps and hinder the returning of injected charge back to needle tip, which may reduce the release of electric mechanical energy. That explains why it is easier to generate electrical tree in XLPE.

Y Murata et al. investigated the volume resistivity and space charge distribution in XLPE/MgO nanocomposite [49] materials. Investigations were made for both XLPE and XLPE/MgO nanocomposite materials. The results indicate the suitability of XLPE/MgO nanocomposite material for HVDC insulation. The applications of XLPE in AC transmission up to a rated voltage of 500 kV have been well studied but its use in 500 kV DC has not yet been brought to realization. In order for developing this application, Electric Power Development Co., Ltd. and J-Power Systems Corp. jointly studied over several years and developed DC 500 kV XLPE insulated cable in the year 2001. Thus, in order for using the XLPE insulation material for DC cable, inorganic filler was used. The inorganic filler selected was nanosized magnesium oxide (MgO). Four materials, XLPE(C) (conventional XLPE insulation for AC cable), XLPE(C)/MgO (nanocomposite material made by mixing XLPE(C) with nanosized MgO), XLPE(S) (specially manufactured XLPE including lower content of cross-linking by-products such as acetophenone), and XLPE (S)/MgO (nanocomposite material which is made by mixing XLPE(S) with nanosized MgO. This material is excellent for DC application.), were used for their study.

The systems under study for the measurement of volume resistivity and space charge distribution were in the form of hot pressed sheet with a thickness of about 100 μm . The nanosized MgO had an average diameter of about several tens of nm. A three-terminal electrode system was used for the measurement of volume resistivity where the diameter of the main electrode was 65 mm. Applied electric fields were 40, 60, and 80 kV/mm, and measurement temperatures were 30, 60, and 90 $^{\circ}\text{C}$. The volume resistivity was evaluated from the leakage current value noted ten minutes after the DC voltage application. The electric field dependence of volume resistivity is at 90 $^{\circ}\text{C}$, and the temperature dependence of volume resistivity under the electric field is of 80 kV/mm. From the results of electric field dependence of the volume resistivity at a temperature of 90 and 60 and 30 $^{\circ}\text{C}$ and temperature dependence of the volume resistivity at an electric field of 80, 40, and 60 kV/mm, the volume resistivity follows the order XLPE(S)/MgO > XLPE(C)/MgO > XLPE(S) > XLPE(C).

Pulsed electroacoustic (PEA) method has been utilized by Y Murata et al. for the determination of space charge distribution. Ambient temperature was used for the measurement and DC electric field of 150 kV/mm was applied to the specimen during space charge measurement and the duration of the measurement was 60 min. The space charge distribution was at 150 kV/mm. These results when compared

with respective base polymer showed that the MgO nanocomposites have greater volume resistivity. The presence of cross-linking by-products such as acetophenone in XLPE(C) reduces the volume resistivity of XLPE and also the presence of the small amount of by-products in XLPE(S) results in its larger volume resistivity than XLPE(C). XLPE(S) and LDPE have almost nearer value of the volume resistivity. The volume resistivity of XLPE(C)/MgO is lower than that of XLPE(S)/MgO and LDPE/MgO. The volume resistivity of XLPE(S)/MgO is almost the same as that of the LDPE/MgO. This indicates that the by-products (which decreases the volume resistivity) and nanosized MgO (which increases the volume resistivity) act synergistically in insulating material. Thus, the nanosized MgO makes the XLPE(S)/MgO material, excellent for DC application. The results from space charge distribution indicate that nanosized MgO prevents the packet-like charge from appearing in the nanocomposite materials at high electric fields. Of all the materials investigated by Murata et al., the XLPE(S)/MgO can be seen to be excellent for DC application.

7 Silicon Carbide Nanoparticles in XLPE Matrix (SiC/XLPE Nanocomposite)

Apart from inorganic oxide, inorganic carbides also prove to be an important nanoparticle in nanocomposites. Wang et al. investigated the dielectric properties, DC breakdown strength, and space charge distribution of XLPE/SiC nanocomposites [50]. Free additive LDPE was the base polymer, and 1, 3, and 5 wt% SiC nanoparticles were used for the studies. Here, the particle size of SiC was maintained at 40 nm, and DCP was used as the cross-linking agent for this nanocomposite. The SEM images of XLPE and SiC/XLPE is shown in Fig. 7 below. This results shows that SiC nanoparticles were well dispersed effectively in the 1 wt% nanocomposite. The concentration of the 3 wt% nanocomposite showed some amount of agglomerations, where as in the 5 wt% concentration, few separated nanoparticles could be detected, which caused nanoparticle agglomerations.

Wang et al. studied the dielectric properties using a Novocontrol ALPHA-A high-resolution dielectric analyzer in the frequency range of 10^{-1} – 10^6 Hz. The results of dielectric measurements of XLPE and XLPE/SiC nanocomposites are given in figure. With increase in the nanoparticle weight percentage, both the real and imaginary permittivity increases whose high value is due to the Maxwell–Wagner interface polarization and also the Gouy–Chapman layers in the nanocomposites. They used the Weibull probability parameters for analyzing the DC breakdown strength. Table 3 shows the Weibull parameters for XLPE/SiC nanocomposites.

This shows that 1 and 3 wt% XLPE/SiC nanocomposites give a higher-scale parameters compared with neat XLPE. However, in the 5 wt% XLPE/SiC nanocomposites, smaller-scale parameters predominate, and this causes the reduction in DC breakdown strength. This decrease is due to the poor distribution of

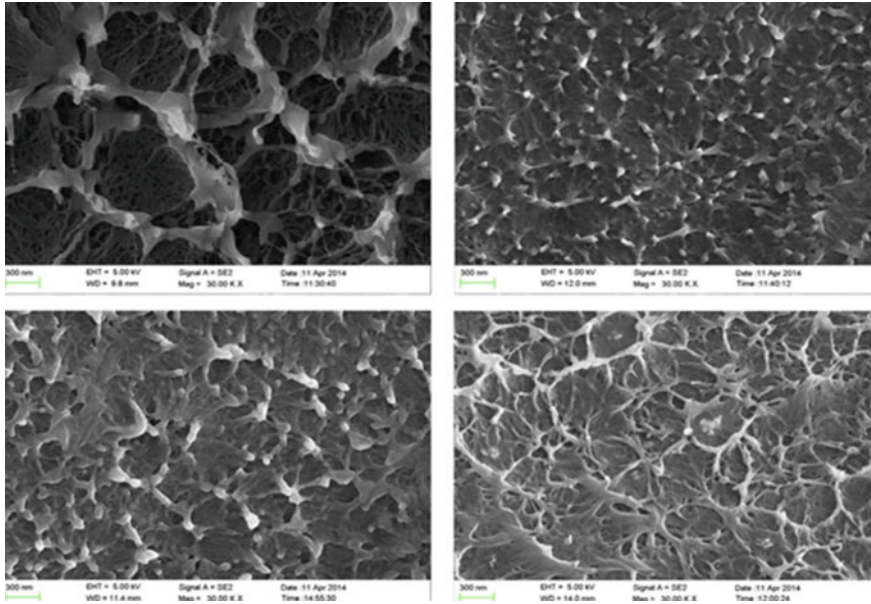


Fig. 7 SEM images of XLPE, 1 wt% XLPE/SiC nanocomposite (right), 3 wt% XLPE/SiC nanocomposite (lower left), 5 wt% XLPE/SiC nanocomposite (lower right). Adapted from [50]

Table 3 Weibull parameters for XLPE/SiC nanocomposites

	XLPE	XLPE/1 wt% SiC	XLPE/3 wt% SiC	XLPE/5 wt% SiC
β	13.08	24.72	15.97	9.71
A	260.67	331.99	297.19	244.71

Adapted from [50]

nanoparticles in the composite. Tanaka et al. gave a multicore model [51] to explain the sharp value of DC breakdown strength which is applicable in space charge behavior. From this model, nanocomposites with lower concentrations of nanoparticles cannot overlap the Gouy–Chapman diffuse layers due to the greater distance between the nanoparticles which also resulted in the better DC breakdown voltage of 1 and 3 wt% sample than 5 wt% sample. In the 5 wt% XLPE/SiC nanocomposite, nanoparticle concentration was high making it difficult to disperse SiC nanoparticles in the polymer matrix. As a result of agglomeration, an overlapping of the Gouy–Chapman diffuse layer was observed. They performed the space charge studies with a pulsed electroacoustic (PEA) method, and the space charge development was confirmed after the 300, 900, and 1800 s of polarization. From the space charge results given in Fig. 8, it has been found that the 1 wt% XLPE/SiC nanocomposite has minimum and 5 wt% XLPE/SiC nanocomposites has the maximum space charge accumulation.

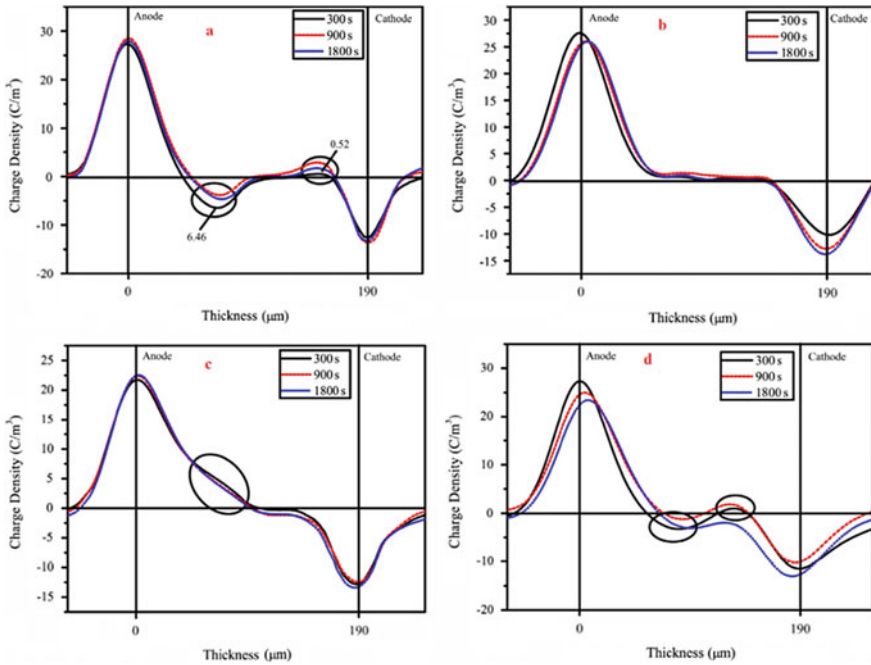


Fig. 8 Space charge behavior of **a** XLPE, **b** 1 wt% XLPE/SiC nanocomposite, **c** 3 wt% XLPE/SiC nanocomposite, and **d** 5 wt% XLPE/SiC nanocomposite. Adapted from [50]

According to Tanaka et al., nanoparticles create deep traps near to the nanoparticle nanocomposite, and each trap could attract a number of electrons and holes. As a result, electrical neutralization occurs when electrons and holes surround a single nanoparticle, preventing charge accumulation in the 1 wt% XLPE/SiC nanocomposite. Also increasing the nanoparticle concentration results in nanoparticle agglomeration affecting the interfacial characteristics between the polymer and nanoparticle. Hence, SiC/XLPE nanocomposite also proves to be an important member of insulation application.

8 XLPE/Clay Nanocomposites

XLPE has proved to be an important insulation material used in nuclear power plant which has been supported by its high melting point, tensile strength, chemical, abrasion, and wear resistance. High voltage, low dielectric loss, resistance to thermal disfigurement, and aging allow them to carry current during different situations like normal conditions, short circuit, emergency, etc., incorporation of clay results on XLPE/clay nanocomposite [52] with unique dielectric properties due to

the multilayered structure of clay. They are a contributing factor to flame retardancy mechanisms.

The XLPE/clay nanocomposites, with different weight composition of nanoparticles up to 5%, were prepared by El Sayed Soliman Said et al. by mixing nanoparticles dispersion in the melted XLPE matrix at a temperature of 120 °C. The nanocomposite material and insulation granules were cooled by water and hot air dried at temperature of 55–65 °C and the obtained materials have been molded at 180 °C in hot press machine for 15 days. Sheets were obtained of thickness 1–2 mm and dimension 20 × 20 cm and pressure 300 Pa. These sheets were divided into two parts in order to study mechanical and electrical characteristics that is dumbbell shape for studying mechanical properties and cubic shape for studying electric properties.

They studied the surface morphology of the nanocomposites using SEM. The SEM of nanocomposite with 1 wt% of nanoclay at different irradiation doses, 50, 100, 300, and 500 KGy as, respectively, showed good mechanical properties. SEM results show that XLPE has a lamellar and spherulitic morphology with an increase in crystallinity and density and hence increases the stiffness and tensile strength of material.

They determined the tensile strength of the nanocomposite of different composition (1%, 2.5%, 4%, and 5%) in the presence and absence of radiation. In the absence of radiation, the tensile strength amounted to (15.69), (21.48), (17.87), (11.06) N/mm², respectively. On the presence of radiation, the tensile strength gradually decreased with increase in the dose of radiation thereby rearranging to cross-linking. This increased the tensile strength for 4 and 5% composition at 100 kGy. Their studies showed that 4% composition gave the best performance of radiation resistance. And 50–300 KGy dose decreases the tensile strength.

They also presented the percentage elongation for different composition. Accordingly the 4% composition had the highest mechanical strength at low doses of radiation. Also, the breakdown strength of nanocomposite increased with incorporation of clay nanoparticles than unfilled one and electrical capacitance and dielectric constant also increased by 20%, for the XLPE/clay nanocomposites at 50 KGy in comparison to pure XLPE. They also presented the comparison of tensile strength, breakdown voltage, and capacitance for neat XLPE and XLPE/clay nanocomposite and showed that the nanocomposite with improved mechanical, electrical, and chemical properties is an ameliorated insulation material for nuclear power plants.

9 XLPE/Al₂O₃ Nanocomposites

The XLPE/ α -Al₂O₃ nanocomposites [53] with its unique qualities have been developed by mechanical blending by Xiangjin Guo et al. and hot press cross-linking where the Al₂O₃ nanosheets were uniformly distributed into a XLPE matrix by the efficient mixing of three constituent namely coated α -Al₂O₃, LDPE,

and dicumyl peroxide (DCP) as cross-linking agent. The presence of Al_2O_3 nanosheets introduced many deep traps that blocked charge injection, reduced charge carrier mobility and conductivity from 3.25×10^{-13} S/m to 1.04×10^{-13} S/m, increased direct current breakdown strength from 220 to 320 kV/mm, and reduced space charge accumulation in XLPE matrix. Further surface modification improved these factors to a larger extent. Al_2O_3 has different crystalline forms with $\alpha\text{-Al}_2\text{O}_3$ showing excellent properties, such as hardness, dimensional stability, good electrical insulation, dielectric constant, and reduced dielectric loss, etc., and the morphological studies were performed using SEM and TEM.

The comparison of DC breakdown strengths of neat XLPE and XLPE/ $\alpha\text{-Al}_2\text{O}_3$ nanocomposites having 0.2, 0.5, 1.0, and 2.0 wt% coated $\alpha\text{-Al}_2\text{O}_3$ is given in Fig. 9. It has been found that in the DC breakdown strength in XLPE/ $\alpha\text{-Al}_2\text{O}_3$ nanocomposites increases with increase in $\alpha\text{-Al}_2\text{O}_3$ percentage.

The space charges distribution of pure XLPE and the XLPE/ $\alpha\text{-Al}_2\text{O}_3$ nanocomposites containing 0.2, 0.5, and 1.0 wt% of $\alpha\text{-Al}_2\text{O}_3$ on the application of a DC voltage of 20 kV/mm is presented in Fig. 10. These space charge studies on neat XLPE and XLPE/ $\alpha\text{-Al}_2\text{O}_3$ nanocomposites using the PEA method show that the presence of $\alpha\text{-Al}_2\text{O}_3$ suppresses the space charge accumulation in the XLPE due to the introduction of number of deep traps in the interface between XLPE matrix and caused by the $\alpha\text{-Al}_2\text{O}_3$. On the application of electric field, such traps capture the electrons or holes injected from the anode or cathode thereby reducing the movement of charge inside the insulation material. As a result of these modified properties, XLPE/ $\alpha\text{-Al}_2\text{O}_3$ nanocomposites may be proved to have important application in the development of materials for HVDC cable insulation.

Yong-Jun Park et al. in 2014 synthesized Al_2O_3 /XLPE nanocomposite using two roll mill [54]. Then the compounds were press-molded at 120 °C for 5 min after

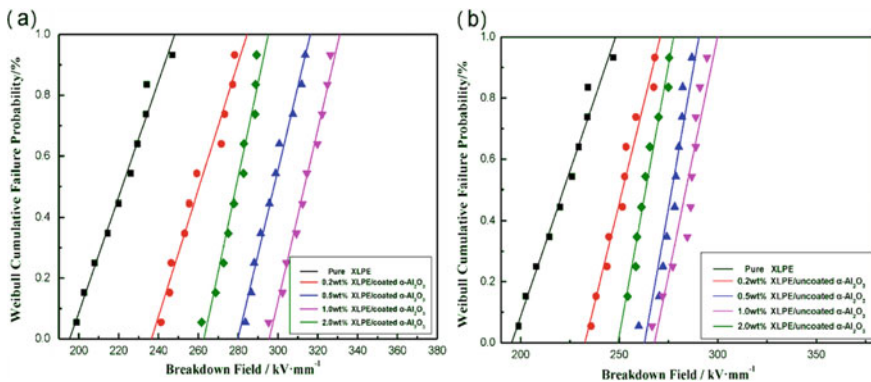


Fig. 9 **a** Weibull plots for comparison of DC breakdown strength of pure XLPE and XLPE/ $\alpha\text{-Al}_2\text{O}_3$ nanocomposites containing 0.2, 0.5, 1.0, and 2.0 wt% coated $\alpha\text{-Al}_2\text{O}_3$ and **b** Weibull plots for comparison of DC breakdown strength of pure XLPE and XLPE/ $\alpha\text{-Al}_2\text{O}_3$ nanocomposites containing 0.2, 0.5, 1.0, and 2.0 wt% uncoated $\alpha\text{-Al}_2\text{O}_3$. Adapted from [53]

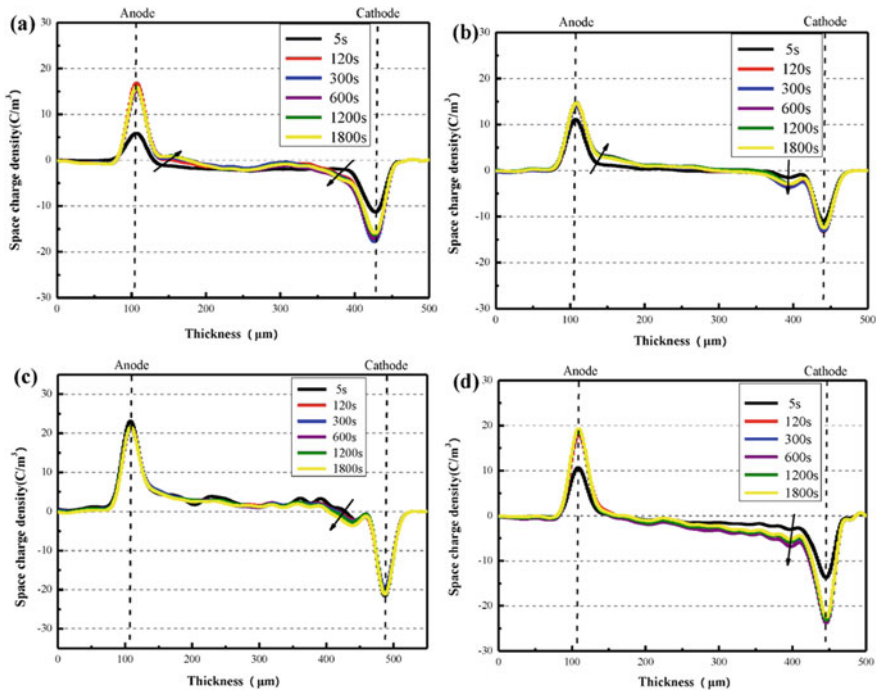


Fig. 10 a The space charge density of pure XLPE varies with the application time of DC voltage (20 kV/mm), b–d the space charge density of the XLPE/ Al_2O_3 nanocomposites containing 0.2, 0.5, and 1.0 wt%— Al_2O_3 varies with the application time of DC voltage (25 kV/mm). Adapted from [53]

that they were cross-linked by hot press at 180 °C for 15 min at a pressure of 10 MPa. It resulted in disk-like structures of 100–120 μm thickness and 100 mm diameter. The resulting samples were then subjected to DC breakdown, DC polarity reversal breakdown, and volume resistivity. The DC breakdown was measured using sphere-to-sphere electrode system at 25 and 90 °C following the IEC60243 standard. The breakdown strength of the systems was studied using Weibull distribution. Their results show that the DC breakdown strength increased with increase in the amount of filler up to 3 phr and the effect of space charge on break down decreased with increase in fillers. They also concluded the increase in volume resistivity with addition if nanofillers and its corresponding decrease with increase in temperature and electric field. Their results were also an additional support to the application of $\text{Al}_2\text{O}_3/\text{XLPE}$ nanocomposite in HVDC insulating materials.

Liang cao et al. presented the conductivity studies of a nano- $\text{Al}_2\text{O}_3/\text{XLPE}$ composite and XLPE filled with polymer from 30 to 90 °C [55]. The current curves of nanocomposites gave similar behavior as ordinary XLPE and different behavior than polymer filled XLPE. Also, the conductivity of polymer filled XLPE was less than nano- $\text{Al}_2\text{O}_3/\text{XLPE}$ composite and ordinary XLPE at temperature lower than

70 °C. These results may be an inspiration for the application of XLPE nanocomposites for HVDC insulations.

10 Other XLPE-Based Nanocomposites

Ahmed Mohammed et al. developed novel nanocomposite as insulation materials for the enhancement of power cables [56]. They focused particularly on thermal conductivity, coefficient of the thermal expansion, and thermal endurance of PVC and XLPE nanocomposites. They result on PVC and XLPE with different nanocomposites like clay, glass beads, and BaTiO₃. Their results proved that glass bead 15 wt% composite has high electric field distribution within insulation due to its low dielectric constant. On the other hand PVC-BaTiO₃ 15 wt% has low electric field distribution due to its high dielectric constant and other composites have electric distribution between these samples. The potential and electric field distribution of the samples were also studied. They inferred that XLPE-Clay 15 wt% nanocomposite showed high electric field distribution and low potential distribution as a result of its reduced dielectric constant and XLPE-Al₂O₃ showed low electric field distribution and high potential distribution as a result of its high dielectric constant. Other members showed electric distribution between these samples. Accordingly addition of nanofillers like clay, BaTiO₃, Al₂O₃ to polymers enhanced their electrical properties and developed their electrostatic field to withstand greater strength. Addition of clay has raised the electric field strength of nanocomposite in comparison to other nano-fillers of fumed silica and Al₂O₃. Hence the composition and type of nanofillers added decides the thickness of the insulating power cables.

Kai Shang Lim et al. in their work reported the effect of nanofillers on the mechanical, physical, dielectric, and thermal properties of XLPE matrix [57]. XLPE having 0.5–2% of ZnO, Al₂O₃, and OMMT nanofillers were prepared by melt mixing with a single screw extruder and then hot press molding. The resulting nanocomposites were subjected to tensile test, water absorption, linear rate of burning, dielectric breakdown strength, thermal stability tests, etc., and the morphological studies were performed using SEM. Their studies showed that the presence of nanofillers increased the tensile strength, elongation at break, Young's modulus, burning rate, dielectric breakdown strength, and decomposition temperature. From their comparison with different nanocomposites, they concluded that Al₂O₃ exhibited the highest properties in comparison to ZnO and OMMT containing nanocomposites. The hydrophilic properties of nanofillers increased the water absorption property with time. However, water absorption increased with time due to the hydrophilic properties of nanofillers.

BX Du et al. investigated the temperature dependence of conductivity and space charge properties of XLPE/graphene oxide (GO) nanocomposites [58]. XLPE samples with varying GO mass fractions of 0, 0.001, 0.01, and 0.1 wt% were prepared. For this the GO prepared by Hummers method with XLPE (mixture of LDPE and dicumyl peroxide) was desiccated for more than 24 h at 80 °C.

Then different concentrations of GO nanoparticles (0, 0.001, 0.01, 0.1 wt%) at 110 °C were blended with XLPE matrix. Finally the resulting was shaped to produce the XLPE/GO nanocomposite of thickness $250 \pm 3 \mu\text{m}$ and maintained in vacuum chamber for 48 h. The related morphological studies were performed using SEM. Using the resulting sample the conductivity, space charge nature and break down strength were analyzed. A three-electrode system was utilized to determine the DC conductivity of the sample. The temperature was maintained between 20 and 150 °C. The space charge studies were conducted using PEA method and the temperature was maintained between 20 and 100 °C DC breakdown strength was conducted using two-copper-ball-electrode system and the power source with a 500 V/s ramping speed was used. They could conclude that the XLPE/GO nanocomposites with GO of 0.01 wt% showed a lower conductivity, space charge accumulation, and higher DC breakdown strength than free XLPE due to the interactions and the deep traps developed by the GO nanoparticles. Also, the temperature dependence of the electrical properties of nanocomposites decreased when appropriate amount of GO was presented. This study also shows that XLPE/GO nanocomposites can also be an important member in HVDC cable insulation.

Guochang Li et al. studied the effect of different concentration of boron nitride nanosheets (BNNSs) on space charge accumulation in XLPE/BNNS nanocomposite [59, 60]. Melt blending method was used to prepare the nanocomposite in an environment of 25 °C and humidity 60 RH%. Finally five different concentrations, 0.1, 0.5, 1, 3, and 5 wt% of BNNS in XLPE were obtained. The results shows a small amount of BNNS (<0.5 wt%) in XLPE matrix that lowers the space charge accumulation due to the formation of deep traps. The increase of BNNS concentration reduces the charge inhibition effect in the system. PEA results show that the accumulated charges increase when the concentration is 1 wt% and for higher concentration the more shallow traps in nanocomposites results in reduced charge accumulation. Hence, these nanocomposites also prove to be better insulation material.

In addition to these nanocomposites, a wide variety of other XLPE nanocomposites has been developed and is also in the course of development to meet the requirements of insulation materials.

11 Conclusion

Apart from these above-mentioned nanoparticles, there are other materials like XLPE/alumina/clay hybrid nanocomposites, Fe_3O_4 , ZnO nanocomposites, semiconductors like PbS- and CdS-based nanocomposites, etc., gaining a great attraction by the scientific world. However, the use of nanocomposite in electrical insulation will increase in the coming days due to its highly encouraging advantages through the addition of small quantities of nanofillers. Also, use of self-healing nanocomposites may acquire the considerable attention in coming days. Furthermore, the interdisciplinary studies in different areas like electrical engineering, computer

science, physics, and chemistry may also accelerate the research to discover new areas of applications. However, the cost reduction and safety issues can also play major roles in its production and implementation.

References

1. Pleša I et al (2016) Properties of polymer composites used in high-voltage applications. *Polymers* 8(5):173
2. Ajayan PM, Schadler LS, Braun PV (2006) Nanocomposite science and technology. John Wiley & Sons
3. Tamboli SM, Mhaske ST, Kale DD (2004) Crosslinked polyethylenes
4. Aljoumaa K, Ajji Z (2016) Mechanical and electrical properties of gamma-irradiated silanecrosslinked polyethylene (Si-XLPE). *J Radioanal Nucl Chem* 307(2):1391–1399
5. Montanari GC et al (2001) Space-charge trapping and conduction in LDPE, HDPE and XLPE. *J Phys D Appl Phys* 34(18):2902
6. Fu M et al (2007) Influence of thermal treatment and residues on space charge accumulation in XLPE for DC power cable application. *IEEE Trans Dielectr Electr Insul* 14(1):53–64
7. Mark JE et al (2005) Inorganic polymers. Oxford University Press on Demand
8. Vahedy V (2006) Polymer insulated high voltage cables. *IEEE Electr Insul Mag* 22(3):13–18
9. Montanari GC et al (2005) From LDPE to XLPE: investigating the change of electrical properties. Part I. Space charge, conduction and lifetime. *IEEE Trans Dielectr Electr Insul* 12(3):438–446
10. Wang Y et al (2016) Effect of nanoparticle surface modification and filling concentration on space charge characteristics in TiO₂/XLPE nanocomposites. *J Nanomater* 2016
11. Lee HWH, Keshavarz M (2004) Nanocomposite materials with engineered properties. U.S. Patent No. 6,710,366, 23 Mar 2004
12. Glatkowski PJ, Arthur DJ (2004) Nanocomposite dielectrics. U.S. Patent No. 6,762,237, 13 Jul 2004
13. Thomas S, Jose JP (2017) 12 Cross-linked polyethylene nanocomposites for dielectric applications. *Advanced composite materials: properties and applications*. Sciendo Migration, pp 527–544
14. Park Y-J et al (2014) Electrical conduction of a XLPE nanocomposite. *J Korean Phys Soc* 65(2):248–252
15. Lewis TJ (1994) Nanometric dielectrics. *IEEE Trans Dielectr Electr Insul* 1(5):812–825
16. Kurnianto R et al (2007) Characterization of tree growth in filled epoxy resin: the effect of filler and moisture contents. *IEEE Trans Dielectr Electr Insul* 14(2):427–435
17. Iizuka T, Tanaka T (2009) Effects of nano silica filler size on treeing breakdown lifetime of epoxy nanocomposites. In: 2009 IEEE 9th international conference on the properties and applications of dielectric materials. IEEE
18. Tanaka T et al (2009) Tree initiation and growth in LDPE/MgO nanocomposites and roles of nano fillers. In: 2009 IEEE conference on electrical insulation and dielectric phenomena. IEEE
19. Tanaka T et al (2011) Dielectric properties of XLPE/SiO₂ nanocomposites based on CIGRE WG D1 24 cooperative test results. *IEEE Trans Dielectr Electr Insul* 18(5):1482–1517
20. Zhang L et al (2014) Effect of nanoparticle surface modification on charge transport characteristics in XLPE/SiO₂ nanocomposites. *IEEE Trans Dielectr Electr Insul* 21(2):424–433
21. Zhang L et al (2014) Effect of nanoparticle surface modification on breakdown and space charge behavior of XLPE/SiO₂ nanocomposites. *IEEE Trans Dielectr Electr Insul* 21(4):1554–1564

22. Zhang L et al (2014) Space charge behavior of XLPE/SiO₂ nanocomposites with nanoparticle surface modification. In: 2014 IEEE electrical insulation conference (EIC). IEEE
23. Lv Z et al (2013) Thickness dependence of space charge in XLPE and its nanocomposites under temperature gradient. In: 2013 IEEE international conference on solid dielectrics (ICSD). IEEE
24. Li S et al (2016) Modelling of dielectric breakdown through charge dynamics for polymer nanocomposites. *IEEE Trans Dielectr Electr Insul* 23(6):3476–3485
25. AshishSharad P, Sathish Kumar K (2017) Application of surface-modified XLPE nanocomposites for electrical insulation-partial discharge and morphological study. *Nanocomposites* 3 (1):30–41
26. Kaihao J et al (2018) Study on dielectric structure and space charge behavior of XLPE/SiO₂ nanocomposites. In: 2018 12th International conference on the properties and applications of dielectric materials (ICPADM). IEEE
27. Han B et al (2016) QM/MD simulations on the role of SiO₂ in polymeric insulation materials. *RSC Adv* 6(1):555–562
28. Balascio JF, Lind T (1997) The growth of piezoelectric alpha quartz crystals. *Curr Opin Solid State Mater Sci* 2(5):588–592
29. De Leeuw NH, Manon Higgins F, Parker SC (1999) Modeling the surface structure and stability of α -quartz. *J Phys Chem B* 103(8):1270–1277
30. Wegener J, Janshoff A, Steinem C (2001) The quartz crystal microbalance as a novel means to study cell-substrate interactions in situ. *Cell Biochem Biophys* 34(1):121–151
31. Ayad MM, Zaki EA, Stejskal J (2007) Determination of the dopant weight fraction in polyaniline films using a quartz-crystal microbalance. *Thin Solid Films* 515(23):8381–8385
32. Rignanese G-M et al (2000) First-principles molecular-dynamics study of the (0001) α —quartz surface. *Phys Rev B* 61(19):13250
33. Koudriachova MV, Beckers JVL, De Leeuw SW (2001) Computer simulation of the quartz surface: a combined ab initio and empirical potential approach. *Comput Mater Sci* 20 (3-4):381–386
34. Del Rosal I et al (2015) Grafting of lanthanide complexes on silica surfaces dehydroxylated at 200 °C: a theoretical investigation. *New J Chem* 39(10):7703–7715
35. Chandrasekhar PS, Komarala VK (2015) Effect of graphene and Au@SiO₂ core–shell nano-composite on photoelectrochemical performance of dye-sensitized solar cells based on N-doped titania nanotubes. *RSC Adv* 5(103):84423–84431
36. Zhao X et al (2011) Investigations on B-doped SiO₂ thermal protective coatings by hybrid sol–gel method. *Thin Solid Films* 519(15):4849–4854
37. Zhang S-S, Zhao Z-Y, Yang P-Z (2015) Analysis of electronic structure and optical properties of N-doped SiO₂ based on DFT calculations. *Modern Phys Lett B* 29(19):1550100
38. Pacchioni G, Vezzoli M, Fanciulli M (2001) Electronic structure of the paramagnetic boron oxygen hole center in B-doped SiO₂. *Phys Rev B* 64(15):155201
39. Zheng X, Liu Y, Wang Y (2018) Electrical tree inhibition by SiO₂/XLPE nanocomposites: insights from first-principles calculations. *J Mol Model* 24(8):200
40. Kresse G, Furthmüller J (1996) Efficient iterative schemes for ab initio total-energy calculations using a plane-wave basis set. *Phys Rev B* 54(16):11169
41. Kresse G, Hafner J (1993) Ab initio molecular dynamics for liquid metals. *Phys Rev B* 47 (1):558
42. Kresse G, Hafner J (1994) Norm-conserving and ultrasoft pseudopotentials for first-row and transition elements. *J Phys: Condens Matter* 6(40):8245
43. Perdew JP, Burke K, Ernzerhof M (1996) Generalized gradient approximation made simple. *Phys Rev Lett* 77(18):3865
44. Blöchl PE, Jepsen O, Andersen OK (1994) Improved tetrahedron method for Brillouin-zone integrations. *Phys Rev B* 49(23):16223
45. Wang Y et al (2016) Study on dielectric properties of TiO₂/XLPE nanocomposites. In: 2016 IEEE international conference on high voltage engineering and application (ICHVE). IEEE

46. Nair AS et al (2016) Influence of nanofillers on resistance to water tree in XLPE nano composite. In: 2016 International conference on circuit, power and computing technologies (ICCPCT). IEEE
47. Li X et al (2014) Influence of organic intercalants on the morphology and dielectric properties of XLPE/montmorillonite nanocomposite dielectrics. *IEEE Trans Dielectr Electr Insul* 21 (4):1705–1717
48. Yani W et al. The effect of nano-MgO addition on grounded DC tree in cross-linked polyethylene
49. Murata Y et al (2008) Investigation of space charge distribution and volume resistivity of XLPE/MgO nanocomposite material under DC voltage application. In: 2008 International symposium on electrical insulating materials (ISEIM 2008). IEEE
50. Wang Y, Wang C, Xiao K (2016) Investigation of the electrical properties of XLPE/SiC nanocomposites. *Polym Testing* 50:145–151
51. Tanaka T, Kozako M, Fuse N, Ohki Y (2005) Proposal of a multicore model for polymer nanocomposite dielectrics. *IEEE Trans Dielectr Electr Insul* 12:669
52. El-kattan WA-E et al (2019) A reduced gamma radiation effects on the electrical insulating cables using XLPE/clay nanocomposites. *J Al-Azhar University Eng Sect* 14(53):1392–1402
53. Guo X et al (2020) Investigation of the space charge and DC breakdown behavior of XLPE/ α -Al₂O₃ nanocomposites. *Materials* 13(6):1333
54. Park Y-J et al (2014) DC conduction and breakdown characteristics of Al₂O₃/cross-linked polyethylene nanocomposites for high voltage direct current transmission cable insulation. *Japanese J Appl Phys* 53(8S3):08NL05
55. Cao L et al (2019) Conductivity of HVDC cable insulation materials: case study between XLPE nanocomposite and polymer filled XLPE. In: 2019 2nd International conference on electrical materials and power equipment (ICEMPE). IEEE
56. Mohamed A, Mobarak Y (2011) Novel nanocomposite insulation materials for the enhancing performance of power cables. In: 21st International conference on electricity distribution, France, Frankfurt
57. Lim KS et al (2019) Properties of nanofillers/crosslinked polyethylene composites for cable insulation. *J Vinyl Addit Technol* 25(S1):E147–E154
58. Du BX et al (2020) Temperature-dependent DC conductivity and space charge distribution of XLPE/GO nanocomposites for HVDC cable insulation. *IEEE Trans Dielectr Electr Insul* 27 (2):418–426
59. Li G et al (2019) Effect of BN nanosheet concentration on space charge characteristics in XLPE/BNNS nanocomposites. *Mater Res Exp* 6(11):115080
60. Li G et al (2020) DC breakdown characteristics of XLPE/BNNS nanocomposites considering BN nanosheet concentration, space charge and temperature. *High Voltage* 5(3):280–286